PSFC/JA-08-19

Cryostat Optimization Through Multiple Stage Thermal Shields

C. Miles, L. Bromberg, J. Minervini
and P. Michael

MIT Plasma Science and Fusion Center

July 11, 2008

Supported in part by a grant from the MIT Energy Initiative

Abstract

Thermal radiation and conduction through structural elements represent a large heat input to the cryogenic environment, especially for cryostats with a large surface area such as those for superconducting transmission lines. In this paper, we discuss methods of decreasing the refrigerator power when the inner cryostat is near liquid nitrogen temperature and the outer cryostat is at room temperature. The use of multiple shield temperature stages is described.

I. Introduction

Progress in high temperature superconductors has opened up superconducting applications that otherwise have been economically unattractive. [4] One such application is power transmission, where the use of liquid nitrogen coolant substantially simplifies the cryogenic requirements. The US Department of Energy has co-funded three substantial demonstrations of the use of HTS in AC transmission lines. [2]

For transmission applications, the cryostat losses are dominated by distributed thermal loads, as the losses in the current terminations are small compared with distributed losses along the superconducting transmission line. In these applications the lines operate at relatively high voltages and relatively low currents, compared with power distribution cables. This is done to minimize AC current losses in the cable. [5, 9, 1, 8]

A small program at the Plasma Science and Fusion Center at MIT is investigating the potential of using HTS cables for DC transmission, and thus eliminate the AC loses in the conductor. Under these circumstances, thermal radiation over the long length of cryostat represents a substantial and dominant heat input to the cryogenic environment.

Multilayer insulation (MLI) is used to reduce the radiant thermal load to the cryogenic environment. MLI consists of multiple sheets of metalized layers separated by non-conducting spacers. The layers are usually made from a plastic (mylar or kapton), metalized with aluminum on either one or two sides. The concept was initially proposed by Sir James Dewar [6].

Means of minimization of the thermal loses in cryogenic environment have been discussed in the past, mainly for applications to cryogenic environments aboard spacecraft. For that application, an additional major requirement is the minimization of the weight of the system.

In this paper, we investigate the minimization of the refrigeration power for cryostats to be used for transmission and distribution cables using high temperature superconductors.

The cryostat MLI shields are located between the room temperature shell (298 K) and the cold cable shell (66 K), but the radiated thermal load is intercepted at intermediate temperatures with separately cooled heat stations. The use of multiple intermediate temperature stations is analyzed for both thermal radiation and thermal conduction cryogenic loads.

II. Model

The analysis of thermal shield using Multi-Layer Insulation (MLI) is in principle very simple. The ideal system consists of thermally insulated layers, each with a constant emissivity, operated in vacuum.

In this analysis, we simplify the calculations using an ideal model, ignoring certain factors such as perforations in MLI used for supports, lead connections, and conduction across different layers in contact. To meet this condition for conduction, the sheets must have a small thermal conductance in the radial direction. This requires precaution during design, manufacturing, and operation of the system in order to adequately meet these conditions and, thus, to approach the results later mentioned in this paper.

The radiated power to a plane surface with a temperature T_c facing a plane surface at temperature T_h is given by

$$W = \sigma (A_h \varepsilon_h T_h^4 - A_c \varepsilon_c T_c^4)$$

where A_h and A_c are the illuminated areas, ε_h and ε_c are the surface emissivities and σ is the Stephan Boltzman constant.

The emissivity of the surface depends on the nature of the material, the history of the material (strain-hardened or soft, contamination), and thickness. In order to obtain maximum reflectivity, the thickness of the coatings needs to be on the order of a few hundred nanometers. Gold and aluminum are preferred materials.

Another complicating fact is that the emissivity is a function of temperature. Constant emissivity will be investigated first. This implication of varying emissivity will be presented in a later section.

In the presence of N shields between two surfaces (assumed parallel planes in this calculation), the thermal radiation can be shown to be [7]

$$W = A\,\varepsilon\,\sigma\,(T_h^4 - T_c^4) / (N + 1)$$

Under steady state conditions, as there are no convection thermal paths, the power radiated across each vacuum gap between thermal layers is a constant. The heat transferred due to conduction through structural supports will be discussed in a later section.

The proposed method to minimize the power requirement is to place one or multiple temperature stations throughout the thermal insulation, in order to intercept the power from the region of higher temperature. To maintain the temperature of the intermediate station at the given temperature, it is necessary to remove heat. This is done with a refrigerator that operates at the intermediate temperature.

In order to determine the electrical power requirement for the overall refrigerator system, an assumption needs to be made with respect to the efficiency of the refrigerators. In this paper, it is assumed that the refrigerator efficiency is a constant fraction of the Carnot efficiency between 323 K (for air-cooled compressors) and the cold end operating temperature of the refrigerator. A relatively conservative multiple of 5 (i.e., 20% of Carnot efficiency) is used for all refrigerators, independent of temperature and capacity. This is a simplifying assumption as it is known that the fraction of Carnot efficiency for a given refrigerator is a weak function of the refrigerator capacity[10].

The electric power requirement for an individual refrigerator P_E is thus,

$$P_E = 5\, Q/\eta_{Carnot}$$

where $\eta_{Carnot} = T_L/(T_H - T_L)$ is the Carnot efficiency of the refrigerator operating between upper temperature T_H and lower temperature T_L. The total electrical power is the sum of the electrical power of the individual refrigerators.

The minimization function is the electrical power. Alternatively, the minimization function could be the capital cost of the overall refrigeration system, or the cost of ownership (capital and operating costs).

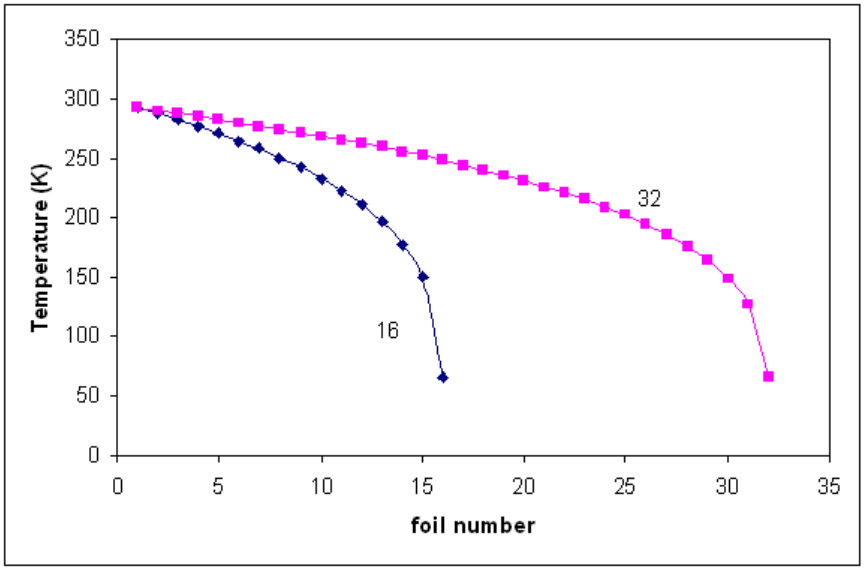

Figure 1. Temperature of the thermal shields for the case of 16 and 32 shields, for ε = 0.07

III. Thermal radiation minimization for constant emissivity

The results for the case of shields with emissivity ε of 0.07 and constant with temperature are presented in this section. Three cases are considered; without intermediate temperature stations, and with 2 or 3 temperature stations.

Results for the case of 16 and 32 shields without intermediate temperature stations are shown in Fig. 1. The temperature profile of the thermal shields is relatively flat at the higher temperature region, with most of the temperature gradient at the lower temperatures.

It is assumed that the upper temperature of the cryostat is 293 K, and the lower temperature is 66 K. Assuming that the inner diameter of the cryostat pipe is 12.7 cm, the thermal load for the case of 32 thermal layers is 0.37 W/m, with an associated electrical power of the refrigerator of 7.32 W/m. It is assumed that the upper temperature of the refrigerator is 323 K (assuming air as the thermal sink).

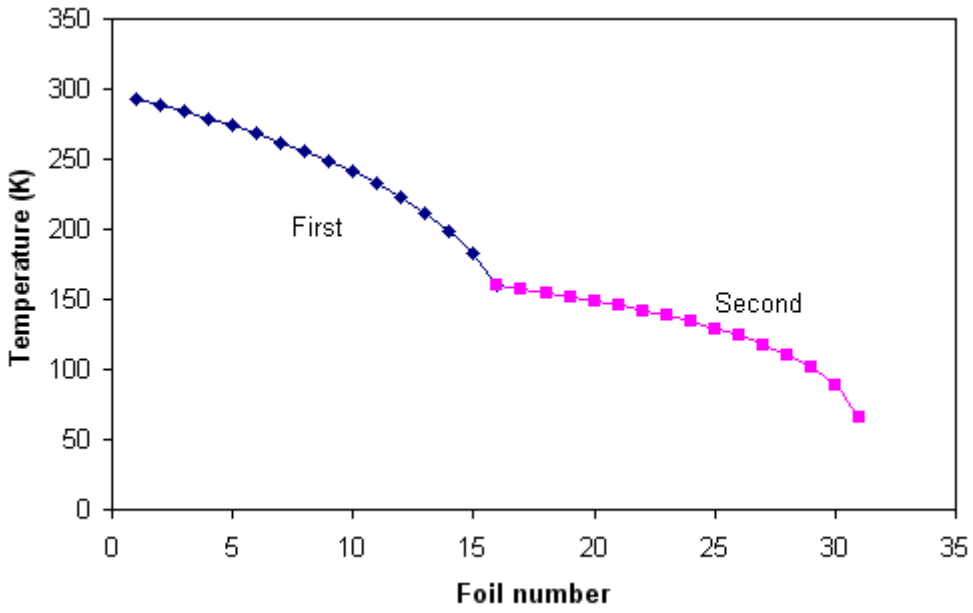

Figure 2. Temperature of the thermal layers for the case of one temperature station, at an intermediate temperature of 160 K.

The case with one temperature station of 160 K located at layer 16 is shown in Fig. 2. As in the previous case, there is a larger temperature gradient at the lower temperatures, for both the upper stage and lower stage.

The thermal load to the 66K refrigerator decreased to less than 0.07 W/m. The associated electrical refrigerator power decreased from 7.3 W/m to 1.2 W/m, or about 80% reduction. Note that it is necessary to cool the intermediate temperature station with a thermal load that is about the same as that of the case of 16 layers without temperature stations, about 0.7 W/m. However, the temperature of operation of the refrigerator is higher, thus decreasing the total electrical power required.

Fig. 3 shows the electrical power requirement for the single stage (7.3 W/m) for 32 layers. The electrical power requirement for the two-stage system is shown separately as a function of the temperature for each temperature station, as well as the total electrical power. The total electrical power minimizes at an intermediate temperature around 180 K, but it is relatively flat. It may be more useful to decrease the size of the lower temperature refrigerator further, at the expense of a slightly larger intermediate temperature refrigerator.

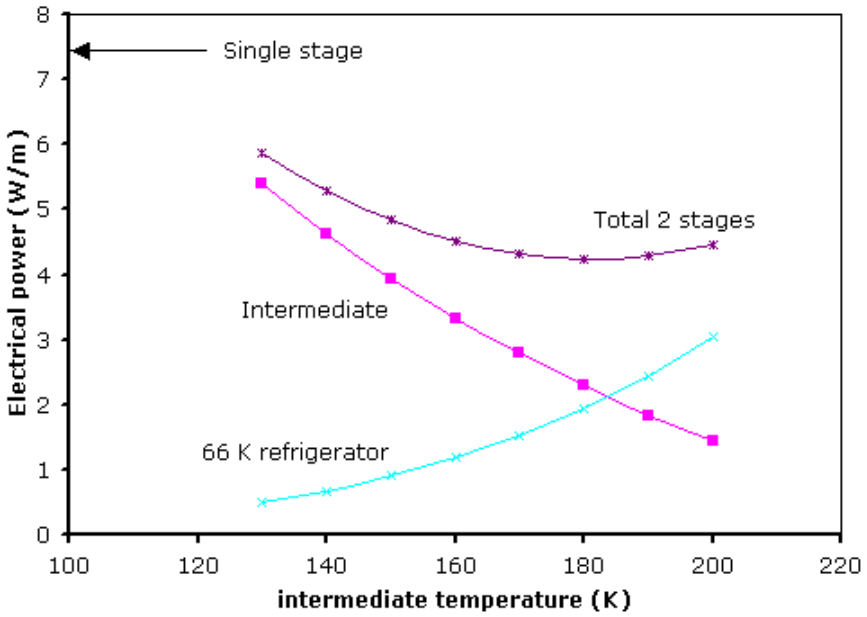

Figure 3. Electrical power required to remove radiation loads for the case of no intermediate temperature station (single stage with 32 layers) and for two stages, as a function of the temperature of the intermediate stage.

As compared with the single stage electrical requirement of about 7.3 W/m, the two-stage system has a room temperature power requirement of about 4.5 W/m, or ~38% decrease.

By subdividing the warm-cold gap into two stages, the load to the 66 K refrigerator was greatly reduced substantially although at the same time, placing a significant load on the 160 K refrigerator. The hypothesis was that this displacement of the thermal load would be beneficial overall. The main driving idea to this hypothesis was that the intermediate refrigerator is capable of handling a larger load since the operating temperature is greater than that of the lower refrigerator. This method of displacing the load to the 160 K refrigerator would hopefully greatly decrease the overall electrical power requirement. The power radiated by the room temperature surface to the colder temperatures is ~ T^4/N. By reducing the number of layers between the room temperature and the intermediate stage by a factor of 2 (16 layers instead of 32 layers), the radiated power intercepted by the intermediate temperature approximately doubled. The higher efficiency of the higher temperature refrigerator more than makes up for the increased radiation, reducing the electrical power, but with a net reduction of only 38% compared to the single stage case.

The case with three stages is described next. In this case, there are two arbitrarily chosen temperatures of the intermediate stages. Fig. 4 shows the temperature of the different layers. It is assumed that there are 16 layers per stage. Note that the overall temperature profile looks much more linear than the one shown in Figure 1.

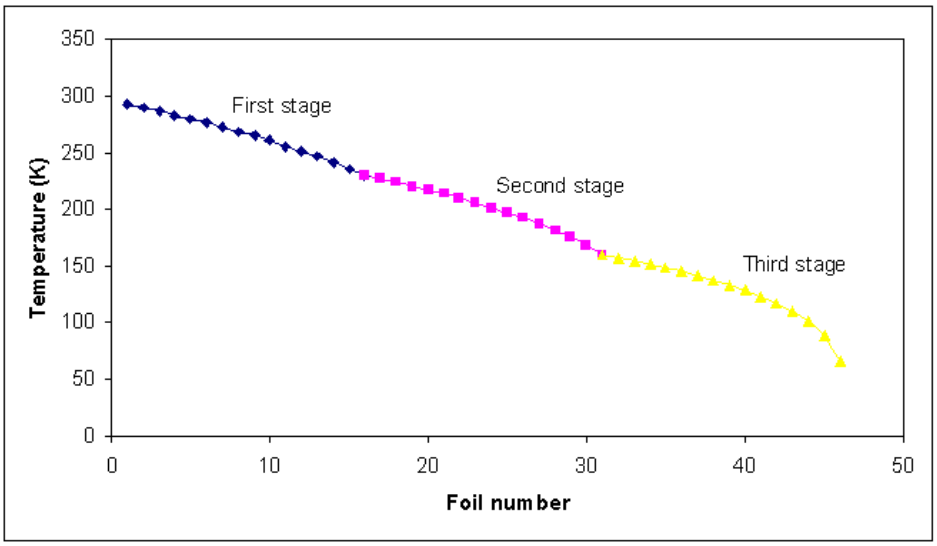

Figure 4. Temperature across the thermal shield for the case of 3 stages, 16 layers per stage.

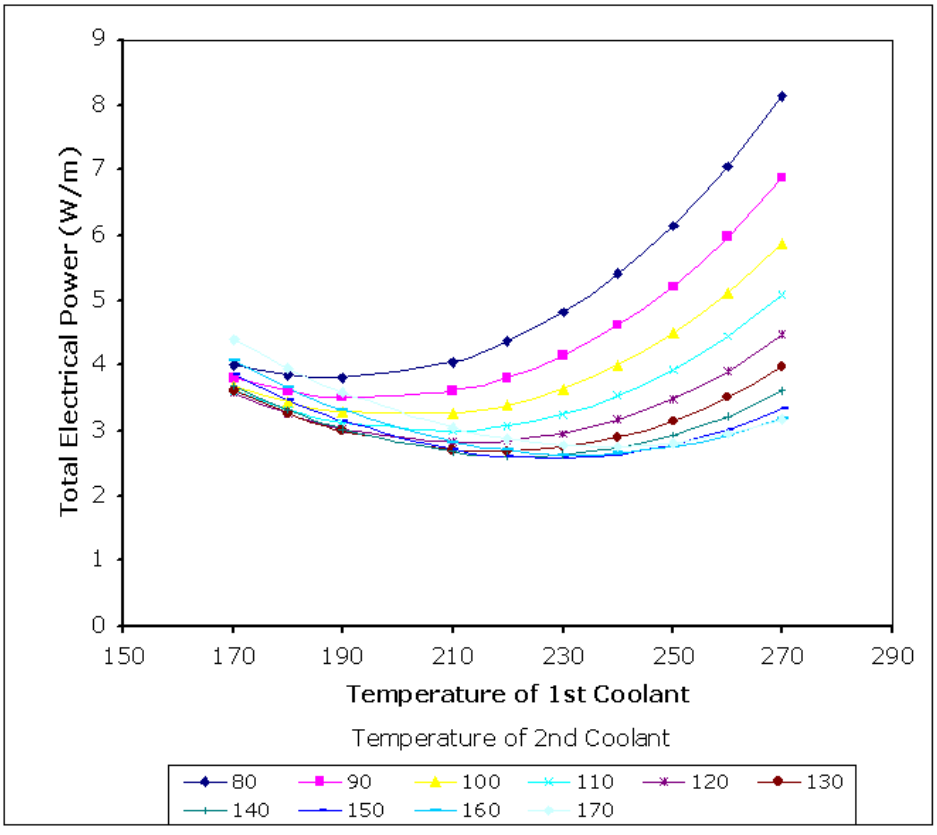

Figure 5. Electrical refrigeration power for the case of 3 stages, as a function of the intermediate stages temperatures.

There is a broad minimum for a temperature of the upper stage of about 230 K and the second stage temperature about 150 K. The electrical power is now reduced to less than 3 W/m. Because the optimum occurs with a temperature of the second stage similar to that of the 2-stage optimization (around 140-150 K), the thermal power to the 66 K environment is similar in both cases. The electrical power reduction is due to a decrease of the power required by the higher temperature stage.

IV. Thermal radiation minimization for temperature dependent emissivity

In this section, the variation of emissivity of the shells due to the variation of temperature is included in the analysis. In this analysis, emissivity is modeled as a decreasing linear function of temperature, which ranges from .07 at 293 K to .058 at 66 K[7].The calculated temperature profiles for the single stage and two-stage models are illustrated in Figures 6 and 7, respectively. From these two plots, it is clear that the variation of emissivity across the shells has a small affect on both models compared to the case with constant emissivity.

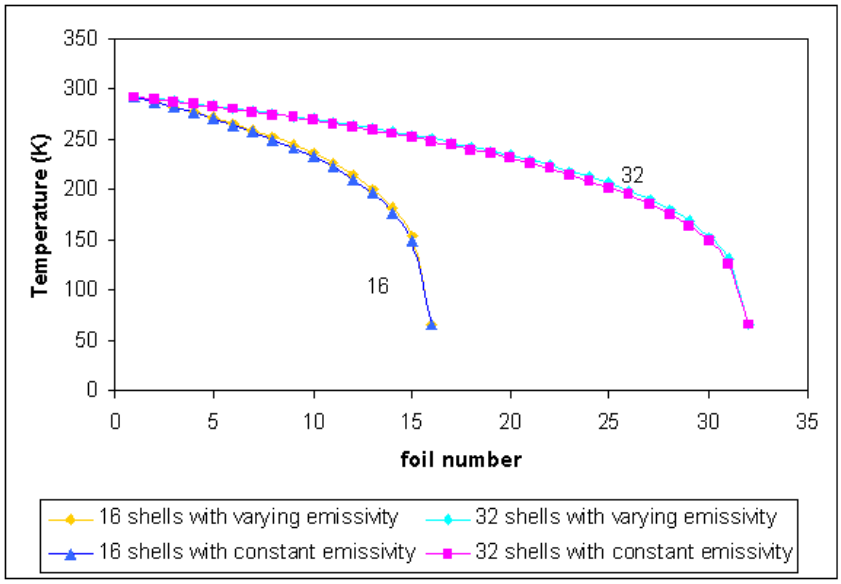

Figure 6. Single stage temperature profiles for temperature dependent emissivity and constant emissivity.

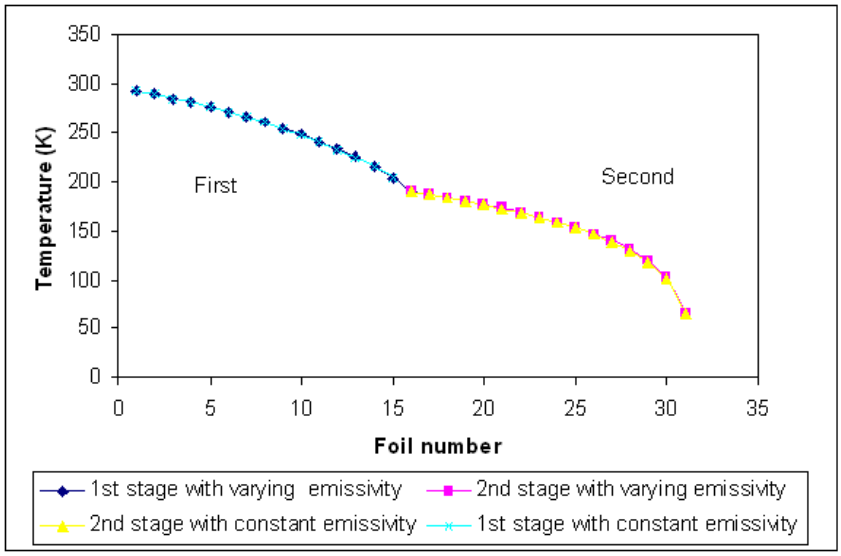

Figure 7. Two-stage temperature profile across shells for temperature dependent emissivity and constant emissivity.

These results show that the analysis in the previous section with constant emissivity over this temperature range is sufficient for understanding these systems.

V. Thermal Conduction through Structural Supports

Another thermal path between the coolant to the surrounding atmosphere is conduction through the structural supports/spacers. The cryogenic load is dependent on the geometry and choice of material of these supports. Two models that differ in both aspects were analyzed.

Models

The first model uses stainless steel tubing, bent into a triangular-like geometry (see Fig. 8). The tube diameter is 2 mm and the wall thickness is 0.25 mm. The inner pipe sits within the triangular support forcing the sides of the triangle to bend. The inner pipe is not welded or attached to the triangular frame to reduce thermal conduction through these contact points. However for this analysis, we use the conservative assumption of perfect thermal contact to give an upper bound to the coolant load.

The second model uses a 1 mm thick triangular sheet of either G-10 or Teflon with a circular cutout for the inner pipe (shown in Fig. 9). The vertices of the triangular sheet are assumed to be in intimate contact with the outer pipe.

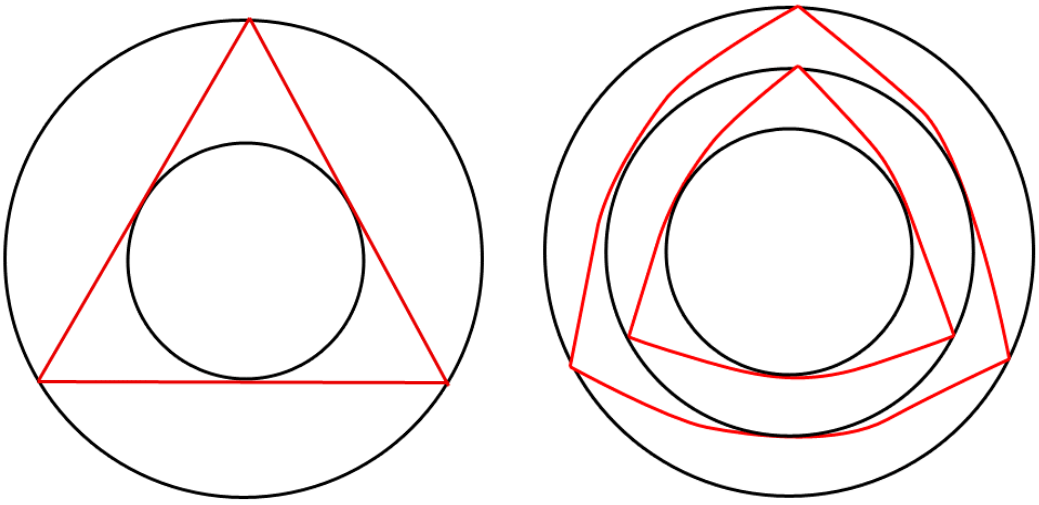

(a) (b)

Figure 8. Stainless steel supports for (a) single stage and (b) two stage cooling.

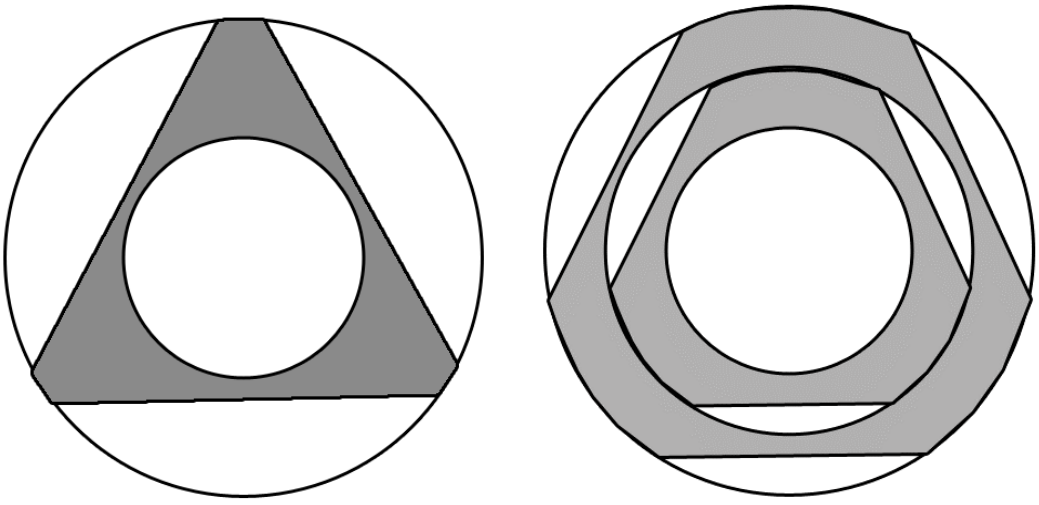

(a) (b)

Figure 9. G-10 or Teflon supports for (a) single stage and (b) two stage cooling.

Analysis

For each model, we compared one stage and two-stage cooling as we described above for radiation. The two-stage cooling design has two supports. One sits between the outer shell and the intermediate shell. The other support sits between the intermediate shell and the inner shell. The temperatures of the outer shell, intermediate shell, and inner shell were 273K, 150K, and 66K, respectively. For both types of supports, the radii of the outer shell, intermediate shell, and inner shell were 80mm, 60mm, and 40mm respectively. The supports were spaced 1 meter apart along the cryostat.

The radiation from the surface of the supports is negligible compared with the conduction load. The rate of heat transfer from one shell to the next is calculated by using the following heat conduction equation along one dimension,

$$Q = -A\,k\,(dT/dx)$$

where Q is the amount of heat flowing through a material per unit time, A is the cross sectional area, k is the thermal conductivity which is function of temperature. The term dT/dx is the spatial temperature gradient. While keeping Q constant (system is in steady state) and A constant, the following equation is obtained [7]:

$$Q=(A/\Delta x)\int k(T)dT$$

Δx is the distance between two thermal contact points. The limits of integration are the temperatures of the two contact points. This one dimensional heat equation works well for analyzing the configuration shown in Fig. 9 for the stainless steel support rods. However, we had to make an approximation for the G-10/Teflon supports by modeling the triangular plate as three 1mm thin rectangular sheets that connect the inner pipe to the outer pipe. Each rectangular sheet had a width equal to the radius of the inner pipe and a length equal to the difference between the two radii. Fig. 10 shows the temperature distribution and heat flux vector field across the support for Teflon. The temperature distribution for G-10 is almost identical.

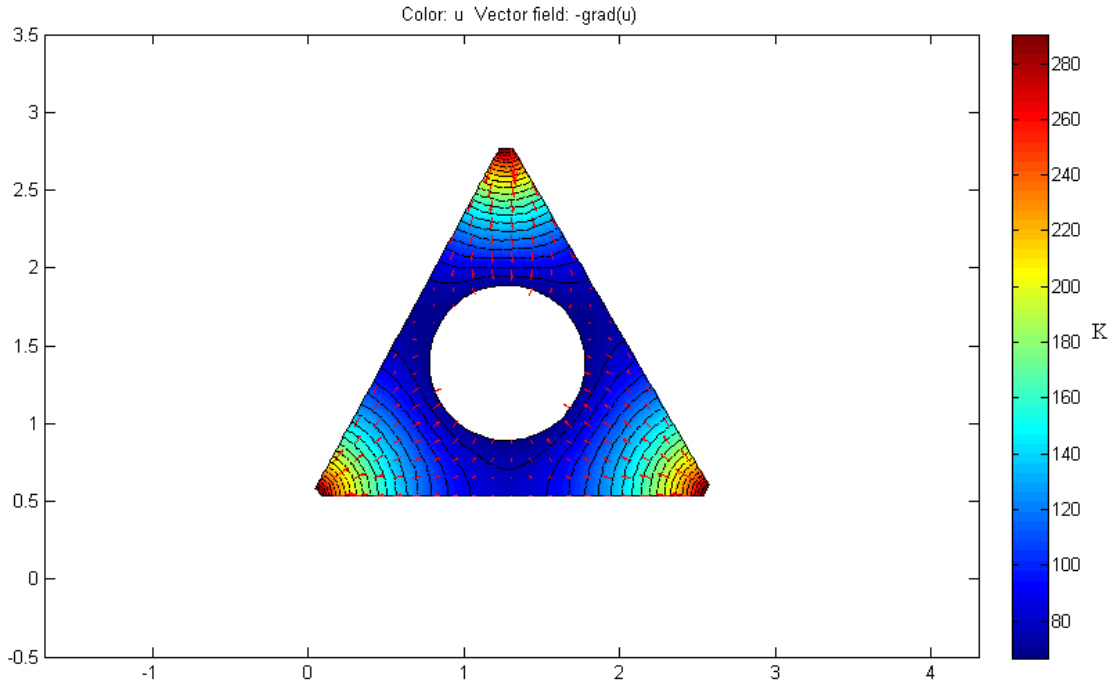

Figure 10. Temperature distribution and heat flux across a Teflon support.

Results

In this analysis, the electrical power per meter was calculated for the models described with a spacing of 1 m between supports. For the G-10 supports, the electrical power required by the refrigeration was about 6.0 W/m for both single stage and two-stage cooling. By using Teflon, the electrical power required by the refrigeration was 1.8 W/m for the single stage cooling and 2.1 W/m for two-stage cooling. For the stainless steel supports, the amount of electrical power for cooling the single stage was about 13.9 W/m. The electrical power for two stages of cooling was about 5.3 W/m.

Recall that these values are the upper bounds of the electrical power required by assuming perfect thermal contact between each support and the shells around it. However, this is not the case in practice. The realistic values are only a fraction of the electrical power for the perfect thermal contact case. Although we are uncertain of the actual electrical power requirement, we can still use the perfect thermal contact electrical power values to compare the two different models. To help compare these results, the values are normalized relative to the electrical power for G-10 single stage cooling.

Table 1.

Electrical Refrigeration Power for Cooling of Structural Supports.

	Electrical Refrigeration Power (W/m)			
	Perfect Thermal Contact		Normalized	
	Single stage	Two stages	Single stage	Two stages
G-10	6.0	6.0	1.00	1.00
Teflon	1.8	2.1	0.30	0.35
Stainless Steel	13.9	5.3	2.32	0.88

VI. Conclusions

This works summarizes efforts to decrease the refrigerator power requirements for cryostats between room temperature and near liquid nitrogen temperatures. This work is relevant to systems operating at temperatures around liquid nitrogen, as well as to systems operating at lower temperature that use MLI thermal shielding between 66 K and room temperature.

It is shown that it is possible to decrease the electrical power requirements of the refrigerator for thermal radiation by about 38% by the use of a two-stage thermal shield, using refrigerator performance that is conservative, for a fixed total number of layers.

The thermal load was displaced from the 66 K refrigerator to the 160 K refrigerator by introducing an intermediate stage cooled by a separate refrigerator. The intermediate refrigerator had higher thermal loading because the number of shells in the gap facing room temperature decreased relative to the case in only a single stage (16 layers vs 32 layers). For this reason, the total electrical power was not reduced by as large of a factor as we had hoped, achieving only about a 38% reduction for the added complexity.

For thermal conduction, the electrical power of the refrigeration system can be decreased by about 60% by the use of a two-stage thermal shield with stainless steel supports. For

G-10 and Teflon supports, it is shown that the electrical power of the refrigeration system remains the same by the use of a two-stage thermal shield.

In the perfect thermal contact case as described in the previous section, the radiation load and conduction load both contribute about equally. However, the realistic value for the electrical power is only a fraction (less than 1/3) of the perfect contact case. Also, if the spacing of the supports is more than 1 m then, the electrical power due to conduction could be further reduced. Therefore, it is reasonable to conclude that radiation is the dominant thermal heat path.

By combining the radiation and conduction analysis, it can be concluded that using Teflon structural supports and a two-stage thermal shield minimizes the electrical power requirement compared to the alternative combinations of the models discussed.

Acknowledgements

This work has been carried out partly under the auspices of the MIT Energy Initiative Seed Fund Program.

References

[1] Demko, J.A. I. Sauers, D.R. James, *et al., Triaxial HTS Cable for the AEP Bixby Project, IEEE Transactions on Applied Superconductivity* **17** 2047-2050

[2] Haught D., *et al., Overview of the U.S. Department of Energy (DOE) High-Temperature Superconductivity Program for Large-Scale Applications, International J Applied Ceramic Tech* **4** 197-202, July 2007

[3] J. A. Demko, J. W. Lue, M. J. Gouge, *et al., Cryostat Vacuum Thermal Considerations for HTS, Power Transmission Cable Systems, IEEE Trans Applied Superconductivity*, VOL. 13, NO. 2, JUNE 2003

[4] Navigant Consulting, http://www.energetics.com/meetings/supercon06/pdfs/Plenary/07_Navigant_HTS_Market_Readiness_Study.pdf

[5] Maguire, J.F, F. Schmidt, S. Bratt, T.E. Welsh *et a*l., *Development And Demonstration Of A HTS Power Cable To Operate In The Long Island Power Authority Transmission Grid, IEEE Transactions on Applied Superconductivity* **17** 2034-7 (2007)

[6] Lady Dewar, Collected papers from Sir James Dewar, Cambridge University Press, Cambridge England (1927)

[7] Weisend II, J. G., *et al., Handbook of Cryogenic Engineering*, Philadelphia, PA, Taylor & Francis, 1998

[8] Sohn, S.H., J.H. Lim, S.W. Yim, *et al., The Results of Installation and Preliminary Test of 22.9 kV, 50 MVA, 100 m Class HTS Power Cable System at KEPCO, IEEE Transactions on Applied Superconductivity* **17** 2043-2046

[9] Weber, C.S, R. Lee, S. Ringo, T. Masuda, *et al.*, *Testing and Demonstration Results of the 350 m Long HTS Cable System Installed in Albany, NY, IEEE Transactions on Applied Superconductivity* **17** 2038-42 (2007)

[10] Strobridge, TR, *Cryogenic Refrigerators, An Updated Survey*, NBS Tech Note 655, US Department of Commerce (1974)